\$ SUPER

Contents lists available at ScienceDirect

### International Journal of Biological Macromolecules

journal homepage: www.elsevier.com/locate/ijbiomac



# The influence of carbon chain lengths on the hydrophobicity characteristics of fiber cellulose / fatty acid composite

Zainab Abdulelah <sup>a</sup>, Zainab J. Sweah <sup>b</sup>, Haider Abdulelah <sup>c</sup>, Ali H. Reshak <sup>d,\*</sup>, Shaymaa A. Al Kareem Shihab <sup>c</sup>, Mohammed Al-Fadhli <sup>e</sup>, Ban Hamdan Al-Mulla <sup>f</sup>

- <sup>a</sup> Department of Chemistry, Science College, University of Basrah, Basrah, Iraq
- <sup>b</sup> Department of Chemistry and polymer Technology, Polymer Research Centre, University of Basrah, Iraq
- <sup>c</sup> Department of Material Science, Polymer Research Centre, University of Basrah, Iraq
- <sup>d</sup> Physics Department, College of Science, University of Basrah, Basrah, 61004, Iraq
- e College of Science, University of Lincoln, Lincoln, LN6 7TS, UK
- <sup>f</sup> Centre of Electrical Energy Systems, Institute of Future Energy, Universiti Teknologi Malaysia, Johor Bahru, Malaysia

### ARTICLE INFO

### Keywords: Waste cellulose Fatty acid Carbon chain length Sustainable coatings Hydrophobicity

### ABSTRACT

In this study, long-chain saturated fatty acid was utilized to modify waste cellulose fibers sheet of Metromilan company for the preparation a hydrophobic composite. To our knowledge, researchers have paid no attention to the effect of carbon chain length in fatty acids used to modify cellulose. In this study, hydrophobic coating was developed using waste fiber cellulose sheet modified with palmitic (PA) and stearic (SA) acids. The method involves immersing fiber cellulose sheet in fatty acids of varying chain lengths to enhance fiber dispersion and enable the formation of modified cellulose sheets. This modified cellulose, in turn, could facilitate the dispersion of fatty acids, resulting in the formation of a hydrophobic coating. In addition, a low-cost device has been created in-house to measure water contact angles (CA). Cellulose sheet neEDX less amount of palmitic acid than stearic acid yielding a smoother film. Cellulose/PA composite exhibits a higher CA of 126.72° and lower moisture absorption versus stearic acid's best CA of 122.57° achieved at 0.06 M concentration. When applied as a coating, it rendered the paper surface hydrophobic. Energy-dispersive X-ray spectroscopy (EDX) confirmed the elements nature of bare cellulose/fatty acid and the reaction between the cellulose sheet and fatty acids (PA; SA) through an increase in carbon atomic % (highest percentage). The cellulose/PA composite reached 1.57 % (0.06 M) and the cellulose/SA composite reached 10.3 % (0.14 M). Fourier transform infrared spectroscopy (FTIR) analysis confirmed the bonding between cellulose and stearic/palmitic acids through appear peaks at 2913 cm<sup>-1</sup> (CH<sub>2</sub>) and 2882 cm<sup>-1</sup> (CH<sub>3</sub>). Scanning electron microscopy (SEM) imaging explained the fibers and acids morphologies of cellulose and their coverage by fatty acid.

### 1. Introduction

Self-cleaning materials refer to surfaces that enable water droplets to slide or roll off, effectively removing dirt and contaminants [1]. This quality is extensively utilized across various sectors, including textiles, marine, optical, automotive, and aerospace industries [2]. The widespread use of petrochemical plastics has raised serious environmental concerns due to their non-biodegradable nature and high ecological toxicity [3,4]. As a sustainable alternative, cellulose offers significant advantages, including abundant availability, inherent biodegradability, and versatile chemical modifiability through its polyhydroxy groups [5].

Nevertheless, despite these benefits, cellulose-based hydrophobic materials still require substantial property enhancements to meet practical application standards with overcoming their inherent hydrophilicity being one of the most critical challenges [6]. Cellulose, a widely available biopolymer, is commonly utilized as the primary material for manufacturing paper products [7]. Various types of wood, containing cellulose content ranging from 45 % to 50 %, serve as the main raw materials for industrial cellulose production [8]. In addition, the cellulose industry boasts a significant production volume, reaching an astonishing 200 million tons annually worldwide [9]. The crystallinity of natural cellulose, which refers to the amount of crystalline material

E-mail address: maalidph@yahoo.co.uk (A.H. Reshak).

 $<sup>^{\</sup>ast}$  Corresponding author.

present, varies from 50 % in cellulose from herbaceous plants to 80 % in tunicate cellulose, and can be modified through physical methods like dry grinding or physicochemical treatments such as acid hydrolysis. [10]. Cellulose fibers feature a substantial number of hydroxyl (OH) groups on their surface, enabling the formation of hydrogen bonds with water molecules. This interaction facilitates the dispersion of water across the surface [11]. Due to its hydrophilic and hygroscopic properties, cellulose has a natural ability to absorb water. Water contact angles observed on smooth cellulose films range from 27° to 47° [12]. Despite being naturally hydrophilic, cellulose offers unmatched benefits as a substrate for superhydrophobic materials. This is due to its abundance, biodegradability, and distinctive physical, chemical, and mechanical properties, which set it apart from commonly used non-renewable materials [13]. The water vapor barrier properties of cellulose films can be effectively enhanced by incorporating hydrophobic compounds such as fatty acids, beeswax, or lipids into the hydrocolloid matrix, achieved either through pre-drying emulsification of these substances with the aqueous hydrocolloid solution or by creating bilayer structures where a hydrophobic layer coats the hydrocolloid base film. Numerous studies have investigated how these hydrophobic additives influence the functional characteristics of edible films [14-18].

Fatty acids feature aliphatic hydrocarbon backbones ending in a carboxyl group. These molecules derive strong hydrophobicity since their chains contain methyl and methylene groups. Hydrophobicity generally increases with fatty acid carbon chain length [19]. Palmitic and stearic acid as the most prevalent saturated fatty acids exhibit key differences impacting their application in material modification. Palmitic acid is cheaper and more available than stearic acid lowering production costs. Thermally palmitic acid (pristine) withstands near 61.2 °C [20] while stearic acid decomposes around 69.3 °C making the second one suitable for moderate heat as shown in [21]. Chain length differs: palmitic acid has 16 carbon atoms versus stearic acid's 18 [22]. Palmitic acid's shorter chain enables denser material surface packing potentially enhancing hydrophobicity and achieving higher water contact angles. Studies such as those by Agrawal et al. [23] demonstrated that shorter fatty acids can improve superhydrophobicity due to better molecular arrangement. Overall palmitic acid offers a cost-effective and thermally stable option that may provide superior hydrophobic characteristics compared to stearic acid. Ban et al. [24] demonstrated that modifying semiconductor with myristic acid a shorter C14 carbon chain fatty acid significantly enhanced superhydrophobicity achieving a maximum contact angle of 166.8°. This result surpassed prior stearic acid studies reaching only 158.3° suggesting C14 carbon denser coating provides superior hydrophobic properties compared to longer-chain acids like stearic acid [22]. Furthermore, Racca et al. [25] found semiconductor coated with myristic acid 14 carbons showed better thermal stability than those coated with stearic acid. This was attributed to short chain providing more active sites.

Current literature lacks a focus on low-cost methods for enhancing the hydrophobicity of cellulose using waste materials. This study fills that gap by demonstrating a simple technique to convert hydrophilic waste cellulose into hydrophobic composites using palmitic and stearic acids with chain lengths of 16 and 18. Our method achieves high water contact angles that exceed those reported in previous studies.

Lie et al. [26] developed a green, catalyst-free method to synthesize highly hydrophobic amidated cellulose (ADC) by grafting fatty acid (oleic acid, 18 carbon atoms) (OLA) onto aminated cellulose via amide bond formation. The unsaturated fatty acid tail of OLA created a hydrophobic barrier in the ADC films, resulting in a CA of 110°. G. Chen et al. [27] studied the impact of oleic acid (OA) on cellulose sulfate (CS) film properties. They observed that incorporating OA increased the surface CA from 64.2° to 94.0° (CS/OA ratio from 1:0 to 1:0.25), indicating enhanced hydrophobicity. Lui. et al. [28] investigated the effect of blending modified pectin/cellulose by fatty acid (Docosanoic acid, 22-carbon atoms) and they found that it significantly increased the hydrophobicity of the composite membranes. Specifically, the highest

CA for the modified membrane was  $97.6^{\circ}$ , much higher than that of the native membrane ( $68.9^{\circ}$ ).

The interaction between hydrophobic substances and water, along with their resistance to wetting, plays a crucial role in various industrial applications, particularly in processes such as water purification [29]. The general principles hydrophobic surfaces also apply to cellulose-based materials with hydrophobic coatings, adhering to two general rules: 1) the coating must possess a suitable surface structure at the micrometer scale, and 2) the coating must exhibit moderately low surface energy chemistry, such as hydrocarbon or fluorine compounds [30]. Gao et al. [31] highlight that long-chain fluorinated polymers release harmful pollutants, driving research toward eco-friendly hydrophobic materials with reduced or zero fluorine content.

This study focused on the development of hydrophobic cellulose/fatty acid composite coatings using one-step immerse mixture technique. The influence of length carbon chains (16, 18 carbon atoms) on the dispersion of hydrophobic fiber cellulose and the effect of fatty acid content on the wettability of the coating were discussed.

### 2. Methodology: Materials and substrate preparation

### 2.1. Materials

Waste cellulose fibers sheet (Raw material, International Fragrance Corporation, Metromilan, Pakistan). Stearic acid ( $CH_3(CH_2)_{16}COOH$ , Segma-Aldrich, Germany). palmitic acid ( $CH_3(CH_2)_{14}COOH$ , Segma-Aldrich, Germany). Ethanol ( $CH_3CH_2OH$ , Scharlau, Spain).

### 2.2. Substrate

Waste cellulose (Raw material) sheet samples were cut into uniform pieces (30 mm  $\times$  10 mm) with thickness 0.299 mm to serve as substrates for coating.

### 2.3. Fatty acid solutions

Stearic and palmitic acids were dissolved in 10 mL of absolute ethanol due to ability to dissolve both acids effectively at varying concentrations (0.007, 0.035, 0.06, 0.14, and 0.25 M). Solutions were stirred for 15 min at room temperature (25  $^{\circ}$ C) to ensure complete dissolution.

### 2.4. Coating procedure

Immersion: Cellulose substrates were immersed in the fatty acid solutions and left to age for 24 h at room temperature, facilitating composite formation. In addition, to ensure adequate cellulose–fatty acid interaction enabling sufficient adsorption and hydrogen-bond-mediated bonding.

### 2.5. Thermal treatment

Samples were then heated at 60  $^{\circ}$ C for 1 h to enhance hydrophobic coating adhesion and to ensure complete evaporation of the solvent. All details are shown in Fig. (1a).

### 2.6. Characterization

Contact angles were measured using a custom-built contact angle meter. This section provides an overview and examination of the overall system scheme with all electronic components and circuits that have been used in the device including the Arduino (Uno) microcontroller, servo motor (Model: SG90) used for moving the surface of the area tester, and the power supply that is used to feed the overall. The system is divided into two parts, which are the electronic circuit and mechanical design which will be discussed, you can follow these steps: 1) Connect

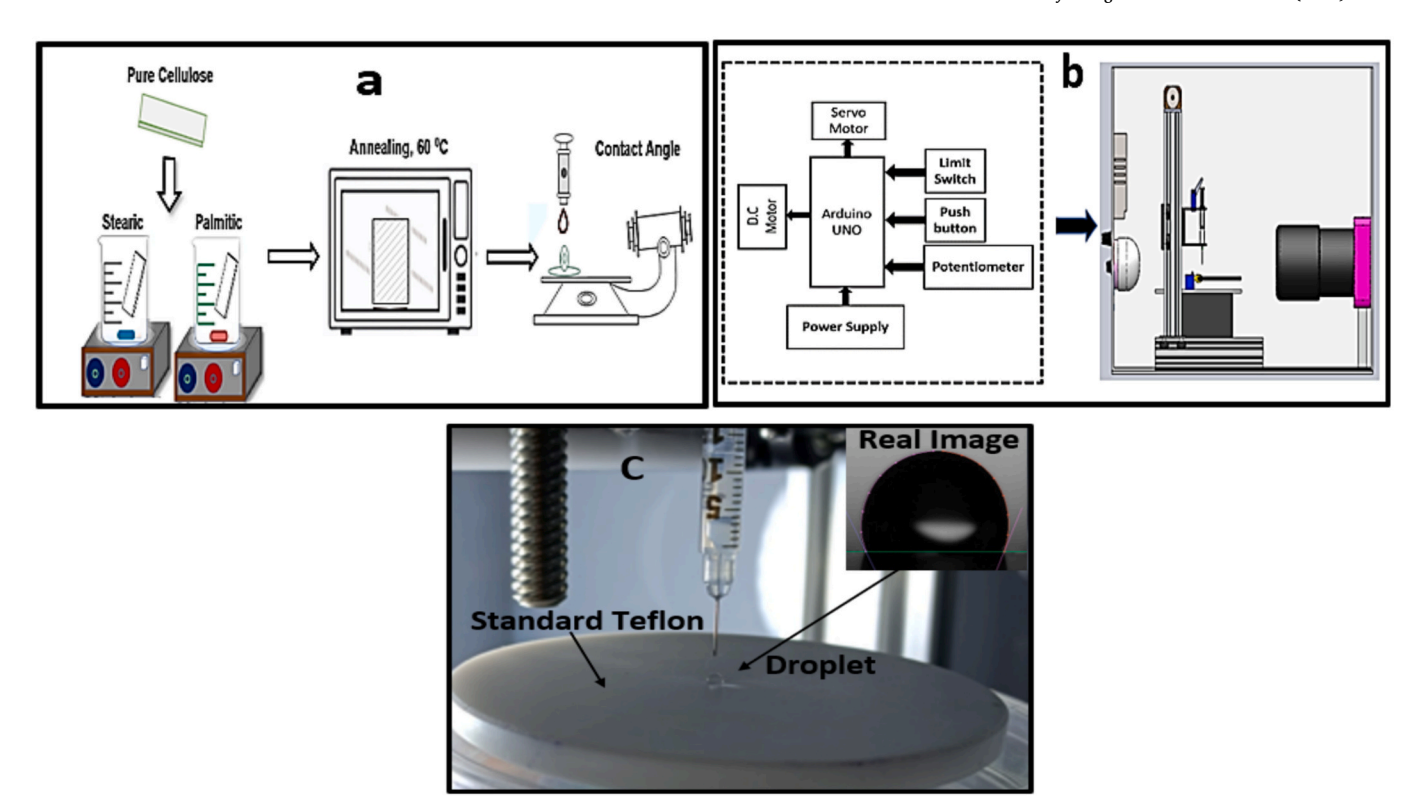


Fig. 1. Experimental set-up of cellulose/fatty acid composite (a), The hardware of control device (b), Normalization of the fabrication system (c).

the DC motor (PG420) to a motor driver module L298N. Connect the push buttons to two digital input pins on the Arduino and the limit switches to two digital input pins as well. Connect the potentiometer to an analog input pin on the Arduino. 2) Write a sketch that reads the state of the two push buttons and the two limit switches using the digital input pins. When the up button is pressed, the DC motor should rotate in one direction until it reaches the up-limit switch. When the down button is pressed, the DC motor should rotate in the opposite direction until it reaches the down limit switch. 3)Use the potentiometer to control the position of the servo motor. Read the value of the potentiometer using the analog input pin and map the value to the range of angles that the servo motor can rotate. Write this angle to the servo motor using the Servo library. 4) Combine the two parts of the sketch to control both the DC motor and the servo motor simultaneously. When the DC motor reaches one of the limit switches, the servo motor should move to a new position. A simple diagram of how to connect a servo motor and other elements to an Arduino. 5) Images of the water droplet have been captured using a microscope camera (51MP 2 K HDMI Industrial Microscope Camera 180× Lens Ring Light) and analyzed using [Ossila] software to determine the CA as shown in Fig. 1(b). Furthermore, the volume of deionized water droplet ( 2 µL) has been deposited carefully on cellulose/fatty acid composite. Finally, the device has been calibrated: A droplet was deposited by the device onto the standard Teflon surface, and the contact angle of the droplet was measured. The measured value was 114.50350° (average), which is an excellent and highly accurate result compared to international standards [32], as shown in the following Fig. 1c.

## 3. Hydrophobicity mechanism and chemical reaction of cellulose/fatty acid

Membrane hydrophobicity relies on constructing hydrophobic surfaces through microstructural design or chemical functionalization. Microstructural design modifies the surface morphology using techniques like co-blending, deposition/coating, or chemical etching. This

creates gaps that increase the energy barrier against liquid penetration achieving hydrophobicity. Such design can be implemented in situ or via post-treatment. The Cassie-Wenzel model explains the mechanism: unlike smooth surfaces where droplets contact closely, rough membrane surfaces trap air molecules forming micro-pockets. These pockets hinder solid-liquid contact and reduce droplet infiltration creating hydrophobicity [33]. Increased surface roughness within limits forms larger air pockets. This synergistically enhances hydrophobicity through hydrostatic pressure, capillary force, and inherent surface properties as shown in Fig. 2a.

Chemical functionality offers an alternative to surface-roughness microstructure design. It achieves hydrophobicity by modifying material surfaces via blending/coating or chemical grafting/crosslinking. These methods introduce chemicals containing hydrophobic groups like aliphatic chains, aromatic rings, organofluorines, or organosilicons which impart low surface energy. These two strategies can also be organically coupled to construct hydrophobic surfaces [34–37]. Fig. 2b shows hydrophobic group action. Weak polarity and minimal hydrogen bonding in these groups reduce affinity for water molecules yielding macroscopic hydrophobic properties. Importantly microstructure and chemical functionality effects interact. Therefore, hydrophobic modification of profiles such as separation membranes usually involves synergistic coupling of both approaches. The characteristics (microstructural and chemical functional) of the CA hydrophobic modification process are summarized in Table 1.

The mechanism reaction by which stearic and palmitic acids attach to the cellulose surface is likely a combination of physical adsorption and hydrogen bonding. Physical adsorption occurs due to Van der Waals forces between the hydrocarbon chains of the fatty acids and the cellulose surface. Xiong et al. [45] fabricated asymmetric membranes via vapor-induced phase separation (VIPS) from a blend of cellulose and styrene–butadiene–styrene block copolymer (SBS), resulting in an SBS hydrophobic layer with a water contact angle greater than 145°. However, these forces are relatively weak and may not be sufficient to create a stable coating. Hydrogen bonding is likely a more significant factor.

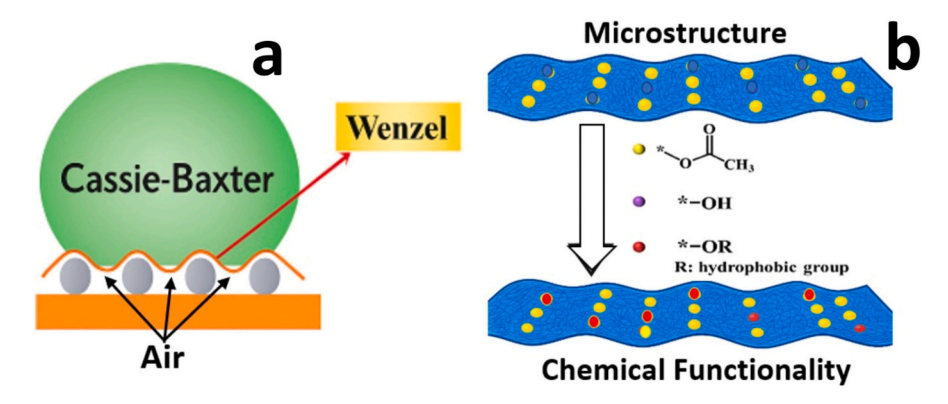


Fig. 2. Hydrophobic interaction mechanism schematic: (a) Surface microstructure (b) Hydrophobic groups.

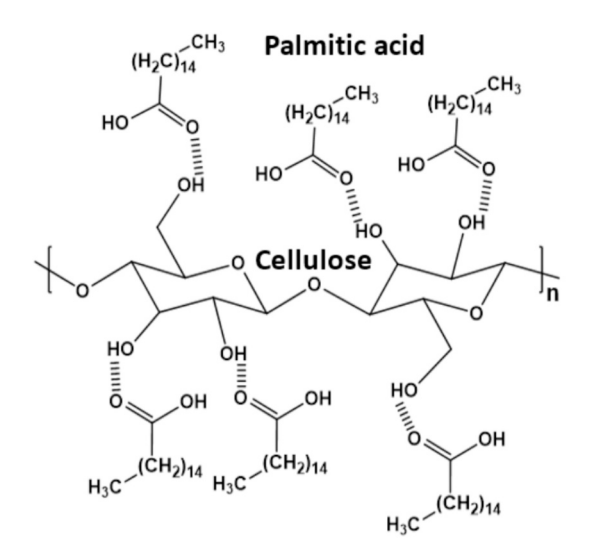
**Table 1**Approaches to enhance hydrophobicity in cellulose.

Polymer type	key substance	Specific process	Contact angle	Ref.
Cellulose triacetate	Fatty alkyl thiols	Thio-Michael click reactions	100 <sup>0</sup>	[38]
Cellulose acetate- polyacrylonitrile	_	Electrospinning	131 <sup>0</sup>	[39]
polylactic acid/cellulose acetate	Polyamidoamine	Blending	$79.9^{0}$	[40]
Cellulose acetate	ZnO	Electrospinning	124 <sup>0</sup>	[41]
Cellulose acetate	Siloxane	Cross-linking	100 <sup>0</sup>	[42]
Cellulose acetate	$SiO_2$	Coating	154 <sup>0</sup>	[43]
Cellulose acetate	Polydimethylsiloxane/ SiO <sub>2</sub>	Coating	157 <sup>0</sup>	[44]
Waste Cellulose	Stearic and palmitic acids	Coating	$126.7^{0}$	This study

The carboxyl groups (-COOH) of the fatty acids can form hydrogen bonds with the hydroxyl groups (-OH) of the cellulose. These hydrogen bonds provide a stronger and more stable interaction than physical adsorption alone. Ganesh et al. [46] fabricated nanofiber membranes by blending cellulose with thermoresponsive poly(N-isopropyl acrylamide) (PNIPAM). At room temperature (23  $^{\circ}$ C), these membranes exhibited superhydrophilicity (WCA  $\approx$  0°), attributed to the inherent hydrophilicity of both polymers and intermolecular hydrogen bonding with water. Upon heating to 40  $^{\circ}$ C, PNIPAM underwent a phase transition. This promoted hydrogen bonding between cellulose and PNIPAM molecules, exposing PNIPAM's hydrophobic main chain and increasing the water contact angle to over 130°. The proposed mechanism reaction is illustrated in Fig. 3.

### 4. SEM analysis

Scanning Electron Microscopy (Axia ChemiSEM, Thermo fisher scientific company, Netherlands) is a valuable tool for examining and comparing the surface characteristics, structure, and diameter of natural and modified cellulose. Fig. 4a shows a typical SEM micrograph of the pristine cellulose fibers, revealing their characteristically flat morphology and the presence of small particulate impurities (*Further details on the magnification are provided in the supplementary file*). The distribution analysis reveals that cellulose was uniformly formed in the shape of fibers, with the highest count observed in fibers of larger diameter, averaging between 10 and 15  $\mu m$ . C. Carrasco et al. and Ding et al. [47,48] SEM investigations of individual cellulose fibers reveal the presence of distinctive surface topographical features such as wrinkles, grooves, and fissures.



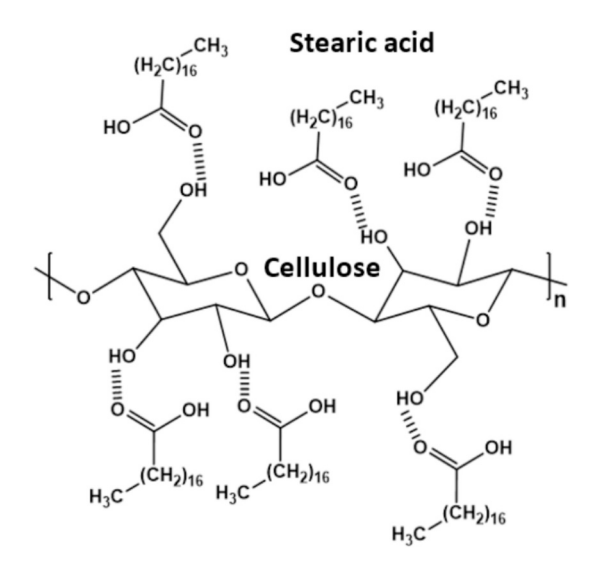


Fig. 3. Demonstrates hydrogen bonding interactions between cellulose and fatty acids.

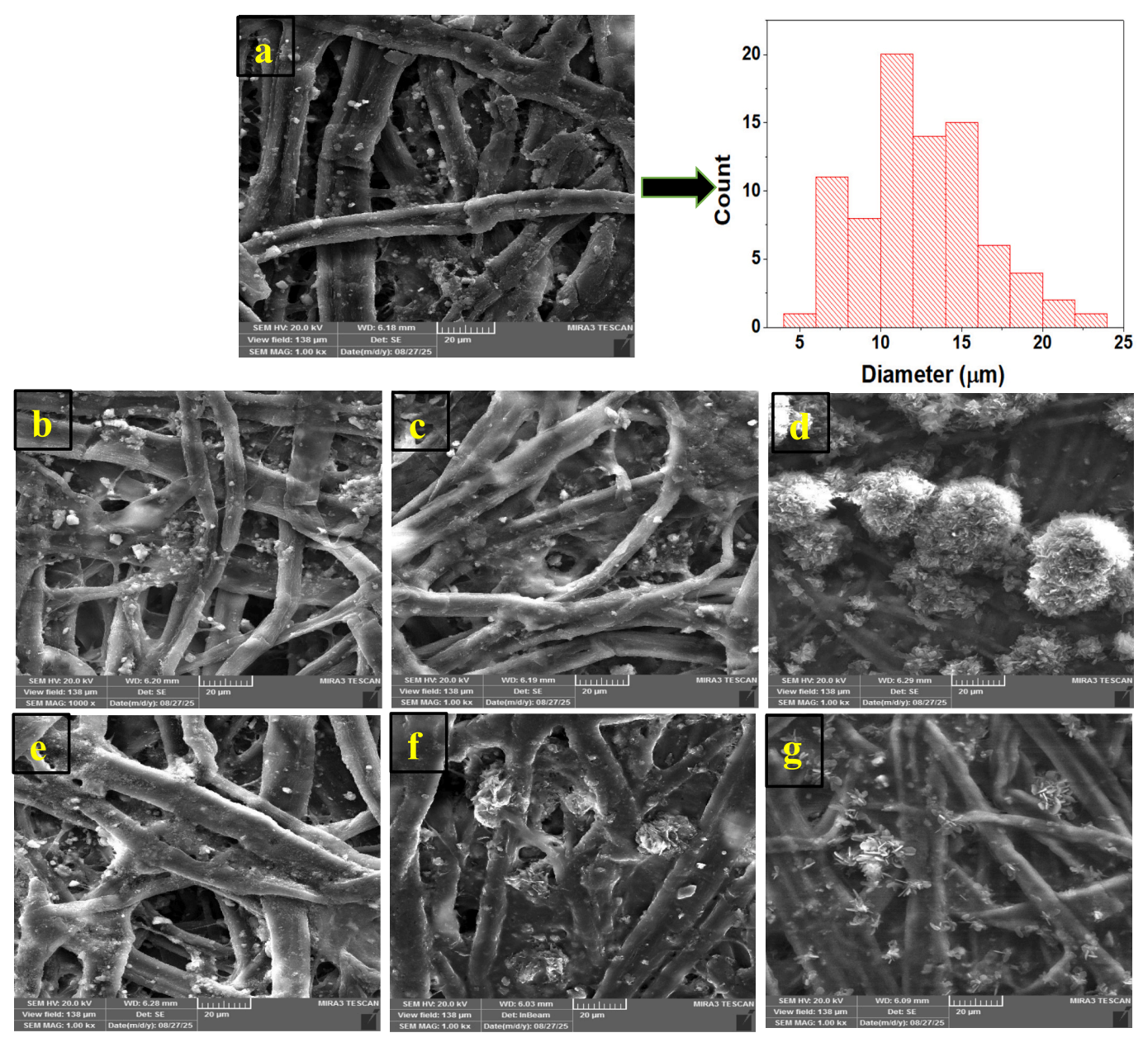


Fig. 4. SEM of pristine cellulose(a), cellulose/ PA (b-d), and cellulose/ SA composites (e-g).

Fig. 4b-g are SEM images of cellulose covered with various concentrations (0.007, 0.06, and 0.14 M) of palmitic and stearic acids under 1kx magnification (Further details on the magnification are provided in the supplementary file). Fig. 4b-d demonstrate that treating cellulose with palmitic acid leads to alterations in the surface morphology, affecting the external appearance of the fibers. Analysis indicated that the cellulose surface underwent specific changes following coating with palmitic acid, which were attributed to the formation of hydrogen bonds. The concentration of palmitic acid significantly affected the fiber's surface topography; a smooth surface was observed at 0.007 M, in contrast to the rough surface generated at 0.06 M as shown in Fig. 4b and Fig. 4c, respectively. At higher concentrations (0.14 M), the fatty acid chains became increasingly entangled, a process that resulted in the formation of aggregated clusters (Fig. 4d). On the other hand, SEM clearly shows that stearic acid covered the cellulose fibers from 0.07 to 0.14 M, and at high molarity (Fig. 4g), clusters appeared due to the entanglement of the chains with each other.

The EDX (XFlash 6110, Bruker, Germany) spectrum was employed to

identify the types of particles that were bonded to the surface of the cellulose fiber sheet. Fig. 5a presents the EDX spectrum for both pure cellulose fibers and the cellulose fibers combined with Palmitic acid samples. The EDX spectrum of the pure cellulose fibers did show the main characteristic peak of carbon (atom %, 12.98), while the EDX spectra of cellulose/palmitic or stearic acid composite samples are clearly showed the increasing in characteristic peaks for carbon from 13.41 reached to 14.55 atom % confirming the existence of fatty acid element on the cellulose fiber surfaces for palmitic samples. It was observed that carbon chain is a major element on the cellulose fibers. However, the carbon atom % of samples stearic acid coated cellulose fibers reached to 23.22 (0.14 M) sample due to the number of carbon chain has 18 atoms greater than palmitic 16 atoms as depicted in Fig. 5b. In addition, other elements such as Flourine, Gallium, Germanium, Selenium, Tantalum, and Arsenic have been appeared due to the cellulose is waste.

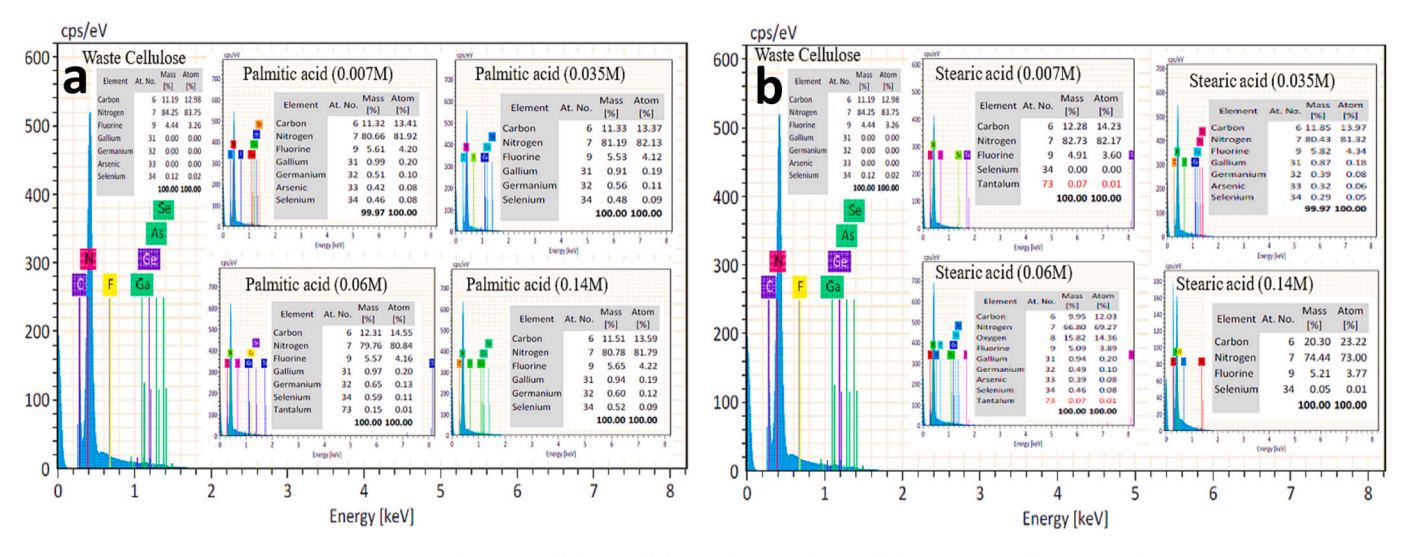


Fig. 5. EDX spectrum of pristine cellulose, cellulose/palmitic acid (a) cellulose/stearic acid composite (b).

### 5. Structural analysis

The X-ray diffractogram (X Pert Pro(MPD) by PanAlytical, Netherland) technique was utilized to thoroughly investigate the crystal structure and evaluate the compatibility of pristine waste cellulose and the cellulose/fatty acids composite at varying concentrations (0, 0.007, 0.06, and 0.14 M). The diffraction peaks were measured over a  $2\theta$  range of  $5^{\circ}$  to  $80^{\circ}$ , with a step size of  $0.04^{\circ}$ min<sup>-1</sup>. Fig. 6 demonstrates that the raw cellulose material and its composites exhibited characteristic diffraction peaks at  $2\theta = 15.6^{\circ}$ ,  $22.5^{\circ}$ , and  $29.4^{\circ}$ , which align with the crystal structure of cellulose, specifically the (1-10), (200), and (004) planes, respectively [49]. A slight shift of the diffraction peak toward lower angles was occurred as the concentration of cellulose/fatty acids increased, indicating changes in cellulose's diffraction lattice planes [50]. Furthermore, the intensity of the  $22.5^{\circ}$  peak increased with higher concentrations of fatty acids (palmitic and stearic), which may be attributed to enhanced crystallinity.

### 6. FTIR analysis

To illustrate the interactions of chemical bonds in the sample, Fig. 7

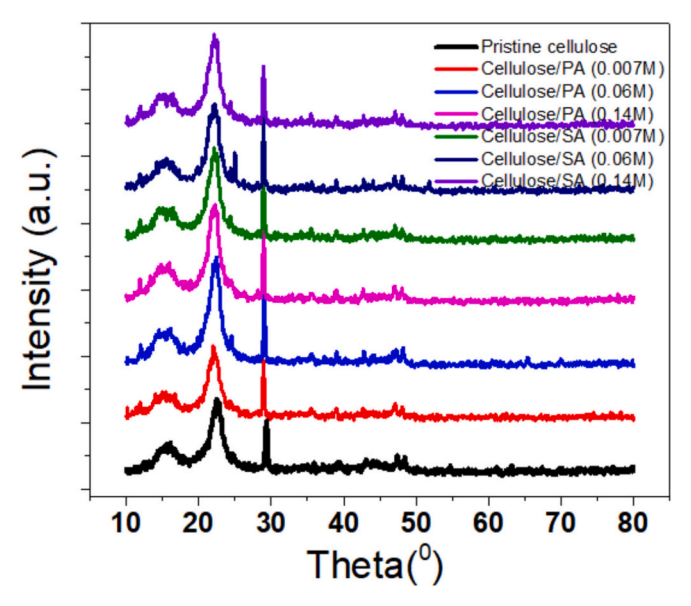


Fig. 6. XRD of pristine waste cellulose and cellulose/fatty acid composites.

(a,b) displays the FTIR (Alpha II, Bruker, Germany) spectra of the raw materials cellulose, stearic, and palmitic acids. The strong broad peak at  $3339~{\rm cm}^{-1}$  has been appeared, which is indicative for the stretching vibrational peak of -OH and hydrogen bond. The characteristic ~1594 cm<sup>-1</sup> peak was attributed to -COOH stretching vibration, While The ~1431 cm<sup>-1</sup> peak was attributed to -OH bending vibration in -COOH (hydrogen bond) [28]. The region between 1000 and 1200 cm<sup>-1</sup> contains numerous absorption bands associated with the stretching vibrations of C-O and C-O-C bonds essential to cellulose structure [51]. Several researchers [52-55] conducted comprehensive FTIR spectroscopy studies on cellulose fibers involved comparing spectra to cellulose standards and determining that absorption bands between 3660 and 2800 cm<sup>-1</sup> and 1650-400 cm<sup>-1</sup> are vital for identifying functional groups. Observed peaks aligned well with spectral data from our cellulose samples. In addition, the presence of fatty chains was confirmed by the double peaks observed at 2913 cm<sup>-1</sup> and 2882 cm<sup>-1</sup> [56]. Their presence confirms stearic acid incorporation into the cellulose structure enhancing its hydrophobic properties.

### 7. Effect of carbon chain length on hydrophobicity

In this study, the number of replicates for each experimental condition should be specified to ensure statistical reliability. Typically, a minimum of three replicates per condition is recommended to account for variability. The change in surface wettability of the samples that have been underwent to modification using fatty acids of different molar masses. The molar mass ratio of stearic and palmitic fatty acids to cellulose was consistently maintained at a surface area of 30 mm  $\times$  10 mm, With the increase in fatty acids content ranged from 0.007 M to 0.25 M. The water droplet on the surface of pristine fiber cellulose is rapidly absorbed within a duration of 10 s due to its exceptional super hydrophilic property. This is primarily attributed to the reactive nature of the hydroxyl groups present in the cellulose structure, which readily interact with water molecules, facilitating swift absorption as shown in Fig. 8a. The effect of the weight ratio of stearic and palmitic acids to cellulose on the hydrophobicity of the samples. The graph visually represents how varying the weight ratio influences the degree of water hydrophobicity exhibited by the modified cellulose as illustrated in Fig. 8(b + c). At a lower molar ratio of 0.007 M, it was observed that the water contact angles measured for the cellulose/SA and cellulose/PA samples were 95.56° and 100.05°, respectively. At a large ratio of 0.06 M, the CA for stearic acid increased to 122.57°, whereas the CA for palmitic acid increased to 126.72°. This suggests that the carboxyl groups of palmitic acid exhibit a greater tendency to rearrange

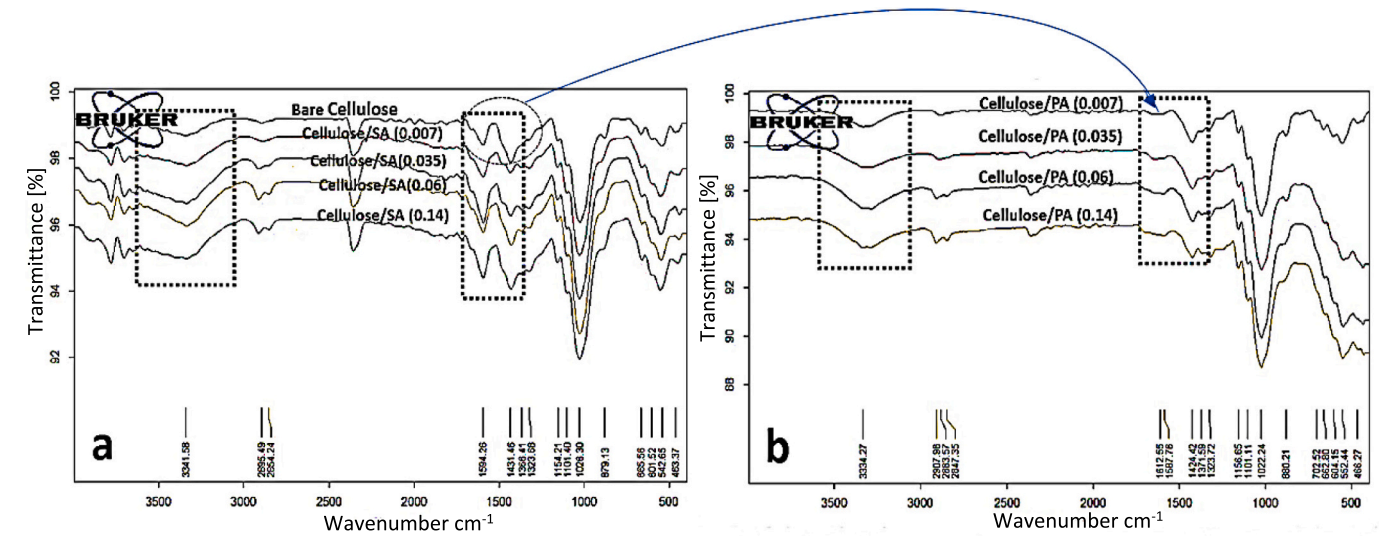


Fig. 7. Shows FTIR analysis of bare Cellulose and Cellulose /Stearic (a), and Cellulose/Palmitic acid (b).

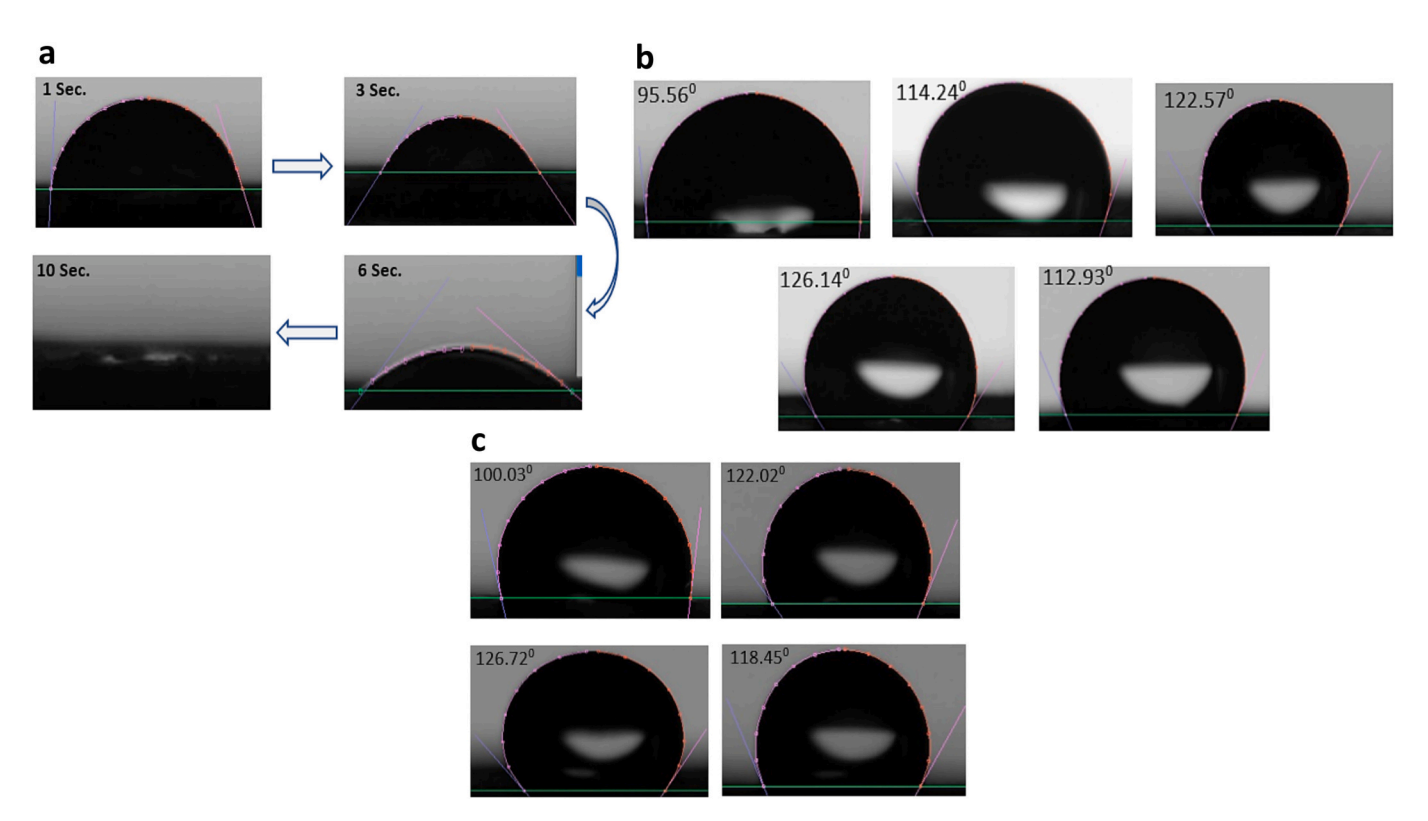


Fig. 8. Contact angle of pristine cellulose (a), cellulose/stearic acid (b), and cellulose/palmitic acid composite (c).

themselves and attach to the active -OH groups on the cellulose surface compared to stearic acid. Increasing the concentrations of fatty acid leads to an excess of carboxyl groups on the cellulose surface. In turn, this excess modifies both the surface free energy and surface roughness. The presence of excess fatty acid on the cellulose surface reduces the surface roughness and can introduce additional hydrophilic fatty acid heads. As a result, the droplet CA is reduced as depicted in Fig. 9. Table 2 presents comprehensive information regarding the CA observed for pure cellulose fiber polymer, as well as its combinations with various fatty acids possessing different carbon chain lengths. Shi et al. [57] address designing surface coatings to protect materials long-term under corrosion. Their coating design's multidimensional nature prioritizes key elements such as surface texture chemical composition and interfacial

adhesion. This thorough strategy enhances coating durability and performance while providing firm technical support for our experimental design and materials selection.

### 8. Conclusion

Scientific and industrial research increasingly focuses on developing environmentally friendly hydrophobic coatings derived from sustainable cellulose. Waste cellulose sheet is combined with fatty acid to form a composite by a simple method. Different length chains of carbon fatty acid such as palmitic and stearic acid have been used to reinforce the hydrophobicity stability. Based on hydrophobicity characterizations, a shorter chain (palmitic acid) shows good results at the lowest amount of

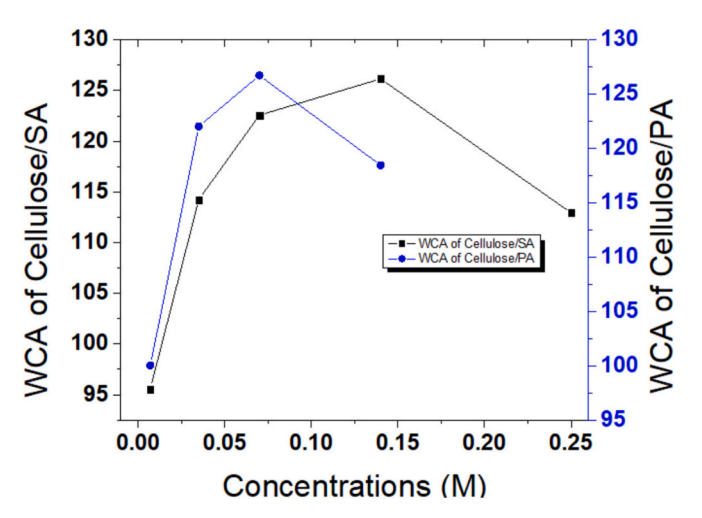


Fig. 9. Contact angle of cellulose with various concentrations of stearic acid, and palmitic acid composite.

Table 2
Various concentrations of cellulose/stearic acid, and palmitic acid composite.

Concentrations (M)	CA of Cellulose/SA (0)	CA of Cellulose/PA (0)
Pristine		
0.007	95.56	100.03
0.035	114.24	122.02
0.06	122.57	126.72
0.14	126.14	118.45
0.25	112.93	

molarity with a CA reaching  $122.72^0$  better than stearic acid of  $114.24^0$  at 0.035 M. In addition, when increasing the molarity both of acids the CA increases to reach  $126.72^0$ ,  $122.57^0$  of palmitic and stearic acid, respectively. Palmitic acid, a highly prevalent and stable fatty acid, possesses a nearly identical structure to stearic acid, making it a potential substitute. Additionally, the shorter chain length of palmitic acid allows for a more compact coverage on fibers, enabling a greater capacity for particle loading within the same volume. This characteristic can contribute to an augmented hydrophobic effect. By coating the walls of fiber cellulose with fatty acids, the proposed process provides an environmentally friendly alternative to their present two-step preservation process, which first involves covering the incense sticks with materials of a polymeric preservative nature, followed by an outer application of fiber cellulose. The proposed process shall reduce the cost and environmental hazards associated with the conventional process.

### CRediT authorship contribution statement

Zainab Abdulelah: Data curation. Zainab J. Sweah: Formal analysis. Haider Abdulelah: Investigation. Ali H. Reshak: Writing – review & editing. Shaymaa A. Al Kareem Shihab: Methodology. Mohammed Al-Fadhli: Software. Ban Hamdan Al-Mulla: Data curation.

### Declaration of competing interest

The authors declare that they have no known competing financial interests or personal relationships that could have appeared to influence the work reported in this paper.

### Appendix A. Supplementary data

Supplementary data to this article can be found online at https://doi.org/10.1016/j.ijbiomac.2025.147939.

### Data availability

No data was used for the research described in the article.

#### References

- [1] S. Somasundaram, V. Kumaravel, Application of nanoparticles for self-cleaning surfaces, in: Emerging Nanostructured Materials for Energy and Environmental Science, 2019, pp. 471–498.
- [2] B.R. Paudyal, S.R. Shakya, Dust accumulation effects on efficiency of solar PV modules for off grid purpose: a case study of Kathmandu, Sol. Energy 135 (2016) 103–110.
- [3] A.A. Koelmans, P.E. Redondo-Hasselerharm, N.H.M. Nor, V.N. de Ruijter, S. M. Mintenig, M. Kooi, Risk assessment of microplastic particles, Nat. Rev. Mater. 7 (2) (2022) 138–152.
- [4] S.B. Borrelle, J. Ringma, K.L. Law, C.C. Monnahan, L. Lebreton, A. McGivern, E. Murphy, J. Jambeck, G.H. Leonard, M.A. Hilleary, Predicted growth in plastic waste exceeds efforts to mitigate plastic pollution, Science 369 (6510) (2020) 1515–1518.
- [5] Y. Pan, F. Wang, T. Wei, C. Zhang, H. Xiao, Hydrophobic modification of bagasse cellulose fibers with cationic latex: adsorption kinetics and mechanism, Chem. Eng. J. 302 (2016) 33–43.
- [6] S. Guzman-Puyol, G. Tedeschi, L. Goldoni, J.J. Benítez, L. Ceseracciu, A. Koschella, T. Heinze, A. Athanassiou, J.A. Heredia-Guerrero, Greaseproof, hydrophobic, and biodegradable food packaging bioplastics from C6-fluorinated cellulose esters, Food Hydrocoll. 128 (2022) 107562.
- [7] B. Thomas, M.C. Raj, J. Joy, A. Moores, G.L. Drisko, C. Sanchez, Nanocellulose, a versatile green platform: from biosources to materials and their applications, Chem. Rev. 118 (24) (2018) 11575–11625.
- [8] M. Ioelovich, Adjustment of hydrophobic properties of cellulose materials, Polymers 13 (8) (2021) 1241.
- [9] E. Malachowska, M. Dubowik, A. Lipkiewicz, K. Przybysz, P. Przybysz, Analysis of cellulose pulp characteristics and processing parameters for efficient paper production, Sustainability 12 (17) (2020) 7219.
- [10] M. Ioelovich, Cellulose: Nanostructured Natural Polymer, LAP Lambert Academic Publishing Sunnyvale, CA, USA2014.
- [11] D.W. Wei, H. Wei, A.C. Gauthier, J. Song, Y. Jin, H. Xiao, Superhydrophobic modification of cellulose and cotton textiles: methodologies and applications, J. Bioresour. Bioprod. 5 (1) (2020) 1–15.
- [12] E. Kontturi, M. Suchy, P. Penttila, B. Jean, K. Pirkkalainen, M. Torkkeli, R. Serimaa, Amorphous characteristics of an ultrathin cellulose film, Biomacromolecules 12 (3) (2011) 770–777.
- [13] J. Song, O.J. Rojas, Paper chemistry: approaching super-hydrophobicity from cellulosic materials: a review, Nord. Pulp Pap. Res. J. 28 (2) (2013) 216–238.
- [14] E. Ayranci, S. Tunc, A method for the measurement of the oxygen permeability and the development of edible films to reduce the rate of oxidative reactions in fresh foods. Food Chem. 80 (3) (2003) 423–431.
- [15] B. Bravin, D. Peressini, A. Sensidoni, Development and application of polysaccharide-lipid edible coating to extend shelf-life of dry bakery products, J. Food Eng. 76 (3) (2006) 280–290.
- [16] M.L. Navarro-Tarazaga, M.A. Del Rio, J.M. Krochta, M.B. Perez-Gago, Fatty acid effect on hydroxypropyl methylcellulose—beeswax edible film properties and postharvest quality of coated 'Ortanique'mandarins, J. Agric. Food Chem. 56 (22) (2008) 10689–10696.
- [17] M.L. Navarro-Tarazaga, A. Massa, M.B. Pérez-Gago, Effect of beeswax content on hydroxypropyl methylcellulose-based edible film properties and postharvest quality of coated plums (cv. Angeleno), LWT-Food Sci. Technol. 44 (10) (2011) 2328–2334.
- [18] M. Soazo, A. Rubiolo, R. Verdini, Effect of drying temperature and beeswax content on moisture isotherms of whey protein emulsion film, Proc. Food Sci. 1 (2011) 210–215.
- [19] J. Sigaux, S. Mathieu, Y. Nguyen, P. Sanchez, J.-G. Letarouilly, M. Soubrier, S. Czernichow, R.-M. Flipo, J. Sellam, C. Daïen, Impact of type and dose of oral polyunsaturated fatty acid supplementation on disease activity in inflammatory rheumatic diseases: a systematic literature review and meta-analysis, Arthritis Res. Ther. 24 (1) (2022) 100.
- [20] G. Fang, H. Li, Z. Chen, X. Liu, Preparation and properties of palmitic acid/SiO2 composites with flame retardant as thermal energy storage materials, Sol. Energy Mater. Sol. Cells 95 (7) (2011) 1875–1881.
- [21] N. Saleema, M. Farzaneh, Thermal effect on superhydrophobic performance of stearic acid modified ZnO nanotowers, Appl. Surf. Sci. 254 (9) (2008) 2690–2695.
- [22] W. Zhu, Y. Wu, Y. Zhang, Fabrication and characterization of superhydrophobicity ZnO nanoparticles with two morphologies by using stearic acid, Mater. Res. Express 6 (11) (2019) 1150d1.
- [23] N. Agrawal, S. Munjal, M.Z. Ansari, N. Khare, Superhydrophobic palmitic acid modified ZnO nanoparticles, Ceram. Int. 43 (16) (2017) 14271–14276.
- [24] B.H. Al-Mulla, H. Abdulelah, A. Nawabjan, S. Hussin, A. Irfan, M.F. Rahman, Fabrication and analysis of ZnO nanoflower and nanorod structures to improve superhydrophobicity using myristic acid, Res. Phys. 67 (2024) 108051.
- [25] L.M. Racca, L.C. Bertolino, C.R. Nascimento, A.M.F. de Sousa, L.Y. Reznik, L. Yokoyama, A.L.N. da Silva, Myristic acid as surface modifier of calcium carbonate hydrophobic nanoparticles, J. Nanopart. Res. 21 (2019) 1–13.

- [26] N. Li, S. Zhang, Y. Liu, V. Nica, S. Coseri, Surficial modification of cellulose with oleic acid via amidation for developing water-resisting property, Ind. Crop. Prod. 203 (2023) 117214.
- [27] G. Chen, B. Zhang, J. Zhao, Dispersion process and effect of oleic acid on properties of cellulose sulfate-oleic acid composite film, Materials 8 (5) (2015) 2346–2360.
- [28] J. Liu, L. Cui, Y. Shi, Q. Zhang, Y. Zhuang, P. Fei, Preparation of hydrophobic composite membranes based on carboxymethyl cellulose and modified pectin: effects of grafting a long-chain saturated fatty acid, Int. J. Biol. Macromol. 222 (2022) 2318–2326.
- [29] S.A. Getaneh, A.G. Temam, A.C. Nwanya, P.M. Ejikeme, F.I. Ezema, Advances in bioinspired superhydrophobic surface materials: a review on preparation, characterization and applications, Hybrid. Adv. 3 (2023) 100077.
- [30] R. Bhattacharyya, Technological Applications of Superhydrophobic Coatings: Needs and Challenges, Indian Institute of Technology Bombay, India, 2009.
- [31] X.H. Gao, J.J. Tang, H.R. Liu, L.B. Liu, Y.Z. Liu, Structure—activity study of fluorine or chlorine-substituted cinnamic acid derivatives with tertiary amine side chain in acetylcholinesterase and butyrylcholinesterase inhibition, Drug Dev. Res. 80 (4) (2019) 438–445.
- [32] P. Chen, Molecular interfacial phenomena of polymers and biopolymers, Taylor & Francis US2005.
- [33] M. Liu, C. Ma, Y. Chen, Y. Wang, J. Xu, Z. Li, L. Deng, L. Zou, J. Wu, H. Wang, Cellulose nonwoven with fast liquid-discharging and anti-return properties: a microplastic-free surface layer for disposable absorbent hygiene products, Chem. Eng, J. 490 (2024) 151291.
- [34] M. Liu, C. Ma, D. Zhou, S. Chen, L. Zou, H. Wang, J. Wu, Hydrophobic, breathable cellulose nonwoven fabrics for disposable hygiene applications, Carbohydr. Polym. 288 (2022) 119367.
- [35] J. Deng, J. Zhang, J. Li, J. He, G. Sun, T. Wang, W. An, Z. Fu, H. Zhao, M. Chen, Polyelectrolyte complex coated cotton fabrics with hydrophobicity, antibacterial activity, and flame retardancy, Macromol. Rapid Commun. 46 (2024) 2400573.
- [36] J. Liu, X. Chen, H. Wang, Fabrication of water/oil-resistant paper by nanocellulose stabilized Pickering emulsion and chitosan, Int. J. Biol. Macromol. 275 (2024) 133609.
- [37] O.T.A. Diejomaoh, A. Lavoratti, J. Laverock, T.T. Koev, Y.Z. Khimyak, T. Kondo, S. J. Eichhorn, Surface modification of cellulose nanomaterials with amine functionalized fluorinated ionic liquids for hydrophobicity and high thermal stability, Carbohydr. Polym. 344 (2024) 122519.
- [38] M. Röhrl, J.F. Ködel, R.L. Timmins, C. Callsen, M. Aksit, M.F. Fink, S. Seibt, A. Weidinger, G. Battagliarin, H. Ruckdäschel, New functional polymer materials via click chemistry-based modification of cellulose acetate, ACS Omega 8 (11) (2023) 9889–9895.
- [39] D. Wang, Y. Yue, Q. Wang, W. Cheng, G. Han, Preparation of cellulose acetate-polyacrylonitrile composite nanofibers by multi-fluid mixing electrospinning method: morphology, wettability, and mechanical properties, Appl. Surf. Sci. 510 (2020) 145462.
- [40] Y. Huang, Y. Jin, B. Wang, H. Tian, Y. Weng, S. Men, Compatibilization and toughening of biodegradable polylactic acid/cellulose acetate films by polyamide amine dendrimers, J. Polym. Environ. 30 (5) (2022) 1758–1771.
- [41] S. Anitha, B. Brabu, D.J. Thiruvadigal, C. Gopalakrishnan, T. Natarajan, Optical, bactericidal and water repellent properties of electrospun nano-composite

- membranes of cellulose acetate and ZnO, Carbohydr. Polym. 97 (2) (2013) 856–863
- [42] G. Stiubianu, A. Nicolescu, A. Nistor, M. Cazacu, C. Varganici, B.C. Simionescu, Chemical modification of cellulose acetate by allylation and crosslinking with siloxane derivatives, Polym. Int. 61 (7) (2012) 1115–1126.
- [43] S. Tasleem, A. Sabah, U.A. Cheema, A. Sabir, Transparent hydrophobic hybrid silica films by green and chemical surfactants, ACS Omega 4 (8) (2019) 13543–13552.
- [44] X. Ji, W. Ji, S. Pourhashem, J. Duan, W. Wang, B. Hou, Novel superhydrophobic core-shell fibers/epoxy coatings with self-healing anti-corrosion properties in both acidic and alkaline environments, React. Funct. Polym. 187 (2023) 105574.
- [45] X. Xiong, Y. Wang, C. Zhong, Preparation of an asymmetric membrane via vapor induced phase separation for membrane distillation, Prog. Org. Coat. 181 (2023) 107590.
- [46] V.A. Ganesh, A.S. Ranganath, R. Sridhar, H.K. Raut, S. Jayaraman, R. Sahay, S. Ramakrishna, A. Baji, Cellulose acetate–poly (N-isopropylacrylamide)-based functional surfaces with temperature-triggered switchable wettability, Macromol. Rapid Commun. 36 (14) (2015) 1368–1373.
- [47] G. Chinga-Carrasco, K. Syverud, Computer-assisted quantification of the multiscale structure of films made of nanofibrillated cellulose, J. Nanopart. Res. 12 (2010) 841–851.
- [48] S.-Y. Ding, S. Zhao, Y. Zeng, Size, shape, and arrangement of native cellulose fibrils in maize cell walls, Cellulose 21 (2014) 863–871.
- [49] A.D. French, Increment in evolution of cellulose crystallinity analysis, Cellulose 27 (10) (2020) 5445–5448.
- [50] H. Bian, Y. Yang, P. Tu, Crystalline structure analysis of all-cellulose nanocomposite films based on corn and wheat straws, BioResources 16 (4) (2021) 8353–8365.
- [51] V. Hospodarova, E. Singovszka, N. Stevulova, Characterization of cellulosic fibers by FTIR spectroscopy for their further implementation to building materials, Am. J. Anal. Chem. 9 (6) (2018) 303–310.
- [52] R. Liu, Q. Li, J. Liu, Y. Duan, T. Gao, Graft copolymerization of MA/(TFEA or TFPM) onto cellulosic fibers for surface hydrophobicity, Cellulose 28 (7) (2021) 3981–3995.
- [53] T. Kawano, Y. Andou, Synthesis and mechanical performance of thermoformable cellulose fatty acid esters using natural soap, RSC Adv. 13 (35) (2023) 24286–24290.
- [54] J. Lease, T. Kawano, Y. Andou, Esterification of cellulose with long fatty acid chain through mechanochemical method, Polymers 13 (24) (2021) 4397.
- [55] W.R. Kunusa, I. Isa, L.A. Laliyo, H. Iyabu, FTIR, XRD and SEM analysis of microcrystalline cellulose (MCC) fibers from corncorbs in alkaline treatment, J. Phys. Conf. Ser. (2018) 012199. IOP Publishing.
- [56] P. Willberg-Keyriläinen, J. Vartiainen, A. Harlin, J. Ropponen, The effect of sidechain length of cellulose fatty acid esters on their thermal, barrier and mechanical properties, Cellulose 24 (2017) 505–517.
- [57] Z. Shi, C. Fang, J. Li, S. Bandaru, M. Liu, L. Zhao, X. Zhang, Multi-dimensional design of slippery liquid-infused coatings empowering long-term corrosion protection for sintered Nd-Fe-B magnets in harsh environments, Small 21 (2025) 2500629.